



Delft University of Technology

## Human back contour modeling for backrest design in future vehicles

Bokdam, Anna; Vledder, Gerbera; Song, Yu (Wolf); Vink, Peter

**DOI**

[10.1016/j.apergo.2025.104700](https://doi.org/10.1016/j.apergo.2025.104700)

**Publication date**

2026

**Document Version**

Final published version

**Published in**

Applied Ergonomics

**Citation (APA)**

Bokdam, A., Vledder, G., Song, Y., & Vink, P. (2026). Human back contour modeling for backrest design in future vehicles. *Applied Ergonomics*, 133, Article 104700. <https://doi.org/10.1016/j.apergo.2025.104700>

**Important note**

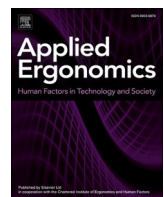
To cite this publication, please use the final published version (if applicable).  
Please check the document version above.

**Copyright**

Other than for strictly personal use, it is not permitted to download, forward or distribute the text or part of it, without the consent of the author(s) and/or copyright holder(s), unless the work is under an open content license such as Creative Commons.

**Takedown policy**

Please contact us and provide details if you believe this document breaches copyrights.  
We will remove access to the work immediately and investigate your claim.



## Human back contour modeling for backrest design in future vehicles

Anna Bokdam, Gerbera Vledder , Yu (Wolf) Song <sup>\*</sup> , Peter Vink

Faculty of Industrial Design Engineering, Delft University of Technology, Landbergstraat 15, 2628CE, Delft, the Netherlands

### ARTICLE INFO

**Keywords:**

Human back contour  
Statistical shape model  
Backrest design

### ABSTRACT

As automated vehicles evolve, seating designs must accommodate a wider range of postures, particularly for non-driving-related activities such as relaxing and sleeping. This study aims to model human back shapes in seated and reclined positions to improve ergonomic seat designs. Human back contour data were collected from 36 participants using a custom measurement device in two setups: a 25° backrest angle and a seat pan angle of 15°, simulating a driving posture, and a 50° backrest angle with the same seat pan angle, representing a reclined posture. Statistical Shape Models (SSMs) were developed to analyze the variability of back contours. The 25° setup exhibited a flatter spinal curve and higher compactness, capturing 79.7 % of the variance with the first principal component (PC1), compared to 74.6 % in the 50° setup. The combined setup balanced these differences, providing a comprehensive model for diverse postures. Overall, PC1, PC2, and PC3 together captured more than 96 % of total contour variance, indicating that variations in back height, neck bending, and lumbar prominence constitute the dominant sources of geometric diversity. These findings offer actionable dimensions for designing ergonomic backrests that support diverse users and postures. Future research should investigate whether implementing these guidelines enhances comfort and should include more diverse populations and a broader range of postures.

### 1. Introduction

The design of automotive seats plays an important role in providing comfort and support during prolonged sitting (Naddeo et al., 2024). The seat contour is often designed to align with the natural shape of the human body. Franz et al. (2011) investigated seat contours in the driver's posture and adapted the backrest and seat pan shapes accordingly, which led to improved comfort. Enlarged contact areas and continuous support along the length of the backrest can help distribute body weight, enhance stability, and reduce pressure concentrations, thereby lowering stress on specific regions and promoting healthy posture (Meakin et al., 2009). However, human body shapes vary, and even for the same individual, different sitting postures can significantly affect the curvature of the lumbar region. For instance, Tsagkaris et al. (2022) showed that sitting often flattens the back, decreasing both thoracic kyphosis and lumbar lordosis compared to standing. These variations present challenges to designing backrests that effectively accommodate diverse postures and body types.

The human spine consists of three distinct curves: the cervical (neck), thoracic (upper back), and lumbar (lower back) regions (Kaiser et al.,

2024). Depending on an individual's sitting height and posture, the thoracic and lumbar regions are most likely to contact the backrest. Studies on spinal angles in upright sitting without a backrest show that the average thoracolumbar angle is approximately 12.01° for males and 9.76° for females, while the lumbar angle is about 8.8° for males and just 0.28° for females (Claus et al., 2016). In other postures, Andersson et al. (1979) found that an increase in the backrest-seat angle had only a minor effect on lumbar lordosis. In contrast, Li et al. (2022) observed that thoracic kyphosis angles increased significantly when transitioning from a standing posture to upright sitting and reading/writing positions, while lumbar lordosis decreased substantially or even disappeared. Using Magnetic Resonance Imaging (MRI), Zemp et al. made measurements on 5 individuals and reported that the mean lumbar, thoracic, and cervical curvature angles were  $29^\circ \pm 15^\circ$ ,  $-29^\circ \pm 4^\circ$ , and  $13^\circ \pm 8^\circ$  in the upright sitting position and  $33^\circ \pm 12^\circ$ ,  $-31^\circ \pm 7^\circ$ , and  $7^\circ \pm 7^\circ$  in a 25° reclined sitting position (Zemp et al., 2013).

The presence of a backrest, particularly lumbar support, might significantly influence spinal curvature. Andersson et al. (1979) found that lumbar lordosis increased proportionally with the addition of lumbar support. A detailed study by Reed and Schneider (M. Reed and

This article is part of a special issue entitled: Occupants Comfort published in Applied Ergonomics.

\* Corresponding author.

E-mail address: [y.song@tudelft.nl](mailto:y.song@tudelft.nl) (Y.(W. Song).

Schneider, 1996) reported that, with a fixed backrest angle of 20° and flexible lumbar support adjustable up to 120 mm above seat pan (M. P. Reed et al., 1995), the lumbar contour prominence measured approximately  $1.5 \pm 5.8$  mm without support and  $10.9 \pm 9.0$  mm with a 40 mm high lumbar support in preferred driving postures. However, the position of the lumbar support along the backrest was not specified. Regarding the height of lumbar support, Carcone and Keir (Carcone and Keir, 2007) demonstrated that a 3 cm lumbar pad effectively provided support and prevented flattening in the lumbar area, underscoring the importance of lumbar support for maintaining comfort during sitting.

In a well-designed seat, the trunk is supported by the backrest, allowing the muscles to relax and the lumbar spine to maintain its natural curve (Varela et al., 2019). However, in seated postures, the back aligns from the buttocks upward, and individual differences in sitting height complicate the use of angular spinal measurements for backrest design. Although substantial effort has been devoted to understanding differences between and within individuals across various postures, significant gaps remain. First contour-based seat shells have been developed using 3D body scans (Franz et al., 2011; Hiemstra-van Mastrigt et al., 2019), and these studies show that shaping the backrest according to human contour can improve pressure distribution and comfort. However, these approaches rely on the mean shape for a single posture rather than developing a generalizable geometric model of the back that spans multiple seated configurations. Lumbar support studies further concentrate on local prominence and its height (Carcone and Keir, 2007; Reed and Schneider, 1996), without modelling the full back contour or how its geometry changes between upright and reclined seating. As a result, a comprehensive geometric model that represents the human back contour across both seated and reclined positions remains lacking, particularly one that extends beyond the limits imposed by conventional vehicle safety constraints.

Second, existing automotive seats are optimized for upright driving

and do not easily accommodate the large changes in spinal and cervical curvature associated with reclined or task-dependent postures. This limitation becomes increasingly relevant in the context of future automated vehicles, where non-driving-related activities (NDRAs) such as sleeping are expected to become more prominent (Cai et al., 2024; Vink et al., 2025). Although the Neutral Body Posture (NBP or “Zero-G”) suggests a trunk-thigh angle of around 128°, this concept focuses mainly on favorable joint-angle configurations rather than on defining the backrest’s geometric contour (Han Kim et al., 2019). Similarly, Vledder et al. (2024) identified a 50° backrest angle as preferred for upright sleeping in vehicles, but the detailed geometric shape of the backrest surface was insufficiently explored.

Addressing these gaps is essential for advancing backrest designs that can support a wide range of postures and activities in future vehicles, including but not limited to automated driving scenarios. Therefore, this paper focuses on two research questions: 1) What is the model of human back shape in seated positions? 2) Is it possible to incorporate more postures, such as sleeping, into the model to better accommodate NDRAs in automated vehicles? By addressing these questions, this study aims to establish a foundation for understanding human back contours across various seating postures and to support the development of adaptable backrest designs that improve comfort across a broad range of in-vehicle activities in the context of automated mobility.

## 2. Materials & methods

### 2.1. Experiment setup

An experiment was conducted at the Comfort Lab of Delft University of Technology to investigate human back contour measurements. A digital measurement device, named the Digital Kyphometer, was specifically developed for this purpose, as shown in Fig. 1 (a). The device

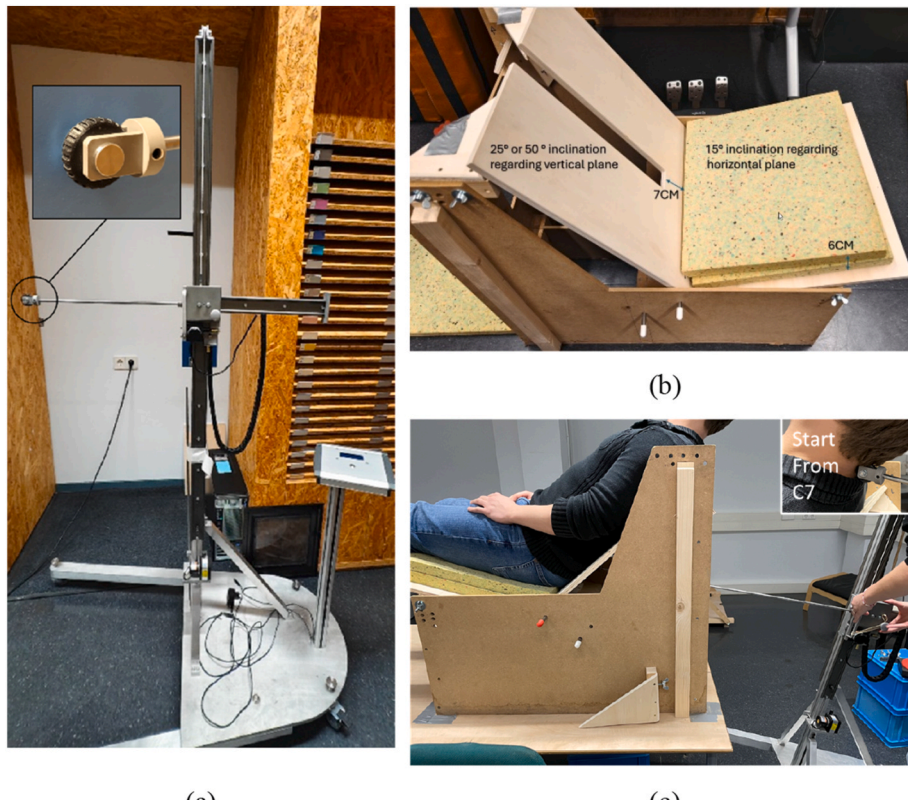


**Fig. 1.** Experiment setup, (a) The Digital Kyphometer used for back contour measurement; (b) the custom experimental seat with a U-shaped slot allowing access for the kyphometer probe; (c) a participant seated during measurement. The inset in the top-right corner indicates the starting landmark at C7.

features a probe mounted on a vertical linear track, enabling it to record both horizontal and vertical movements of a wheel at the end of the probe as it moves along the track. Compared to other measurement methods (de Oliveira et al., 2012; Kandasamy et al., 2021; Nijholt et al., 2016; Voinea et al., 2016), the Digital Kyphometer offers a faster and more efficient way to digitize vertical back profiles.

In addition, a custom wooden seat was fabricated with a 15° seat pan angle and adjustable backrest angles of 25° and 50°, as illustrated in Fig. 1 (b). The 25° backrest angle was selected as it is the most commonly observed angle among drivers (M. P. Reed et al., 2020). In contrast, the 50° backrest angle was chosen based on recent studies suggesting that it provides comfort for sleeping (Gerbera Vledder et al., 2024). A distinctive feature of the seat is the U-shaped slot at the center of the backrest, which allows the probe direct access to the back during measurement. Two layers of foam, totaling 6 cm in thickness, were placed on the seat cushion. The distance from the bottom of the U-shaped slot to the top of the foam is approximately 7 cm, measured along the direction of the backrest. The 7 cm clearance was reserved to ensure that the probe could move freely while accessing the back contour of the participants during measurement. Fig. 1 (c) shows an experiment session, during which the wooden seat was positioned on a table to align with the measurement range of the device. The device was placed behind the seat at an 11° inclination relative to the ground plane, allowing improved access and more accurate back contour measurement.

## 2.2. Participant

The participants consist of 18 males, 17 females, and 1 other gender. The majority (30 participants) are of Western European origin, primarily Dutch nationals. The group also includes individuals from South and Southeast Asia (3), East and Central Asia (1), Eastern Europe (1), and North Africa (1). Table 1 presents the participants' anthropometric data. Fig. 2 shows the distribution of participants based on stature and hip width. The shaded ellipse represents the range between the 5th percentile (P5) and 95th percentile (P95) of the Dutch population for both dimensions, encompassing the central portion of the sample (Dined, 2011).

## 2.3. Protocols

Informed consent was obtained from all participants prior to the study. Anthropometric measurements were collected using a measuring chair to document the participants' physical dimensions following the procedure described by Molenbroek et al. (2017). Subsequently, the kyphometer and the corresponding wooden seat were adjusted to the appropriate settings based on the specified backrest angles, and the origin of the kyphometer measurement was aligned with the top surface of the foam pad. At the 25-degree backrest angle, participants were instructed to look at a fixed point in front of him/her to simulate a driving posture. The researcher then used the kyphometer to measure the back contour, starting from the seventh cervical vertebra (C7) (Wiyanad et al., 2023) to the bottom of the U slot, recording data at 1 cm intervals. This process was repeated three times to ensure consistency and reliability. For the 50-degree backrest angle measurement,

**Table 1**  
Anthropometry of the participants.

	Mean $\pm$ STD	Min	Max
Age	26.4 $\pm$ 10.2	19	66
Stature height (CM)	174.7 $\pm$ 8.7	158.1	191
Popliteal height (CM)	47.2 $\pm$ 3.2	41.6	53
Buttock-knee height (CM)	50.1 $\pm$ 2.4	45.8	55
Sitting height (CM)	89.7 $\pm$ 4.1	80.7	97.5
Hip width (CM)	38.5 $\pm$ 3.4	33.4	48
Weight (Kg)	71.5 $\pm$ 13.5	48	98

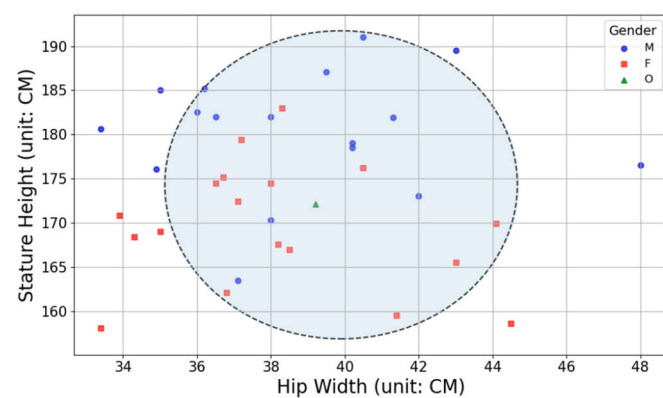


Fig. 2. Distribution of stature and hip width of participants.

participants were instructed to relax as much as possible while seated, and the contour measurement process was repeated under these conditions. The head position was left unrestrained, as occupants tend to vary their head posture while sleeping or relaxing. Arm orientation was left unconstrained to simulate a natural static forward-facing posture.

## 2.4. Data processing

All collected data were documented. Given a set of measured points of a contour of the human back, the acquired data can be represented as

$$P_{CM}^{s,i,m} = \left\{ P_{CM}^{s,j,m,i} \mid i = 0 \dots n^{s,j,m} \right\}$$

where  $P_{CM}^{s,j,m,i}$  represents the  $i$ th measured point of the  $j$ th subject in the  $m$ th try in the measurement coordinate system  $CM$  ( $X_M OY_M$ ) for the  $s$ th setup, and  $n^{s,j,m}$  is the number of points in the pointset  $P_{CM}^{s,i,m}$ . Here  $s = [0, 1]$  referring to the 25° and 50° setups, respectively. An example of  $P_{CM}^{s,j,m,i}$  is the point  $P$  in Fig. 3, and the x and y coordinate of  $P$  is  $[OA, PA]$  in  $CM$ .

As the measurement was conducted in 25° and 50° backrest angles, the distances between point  $P$  and each backrest have more meaning regarding the shape of the human back contour. Therefore, two coordinate systems  $C_{25}$  ( $X_{25} OY_{25}$ ) and  $C_{50}$  ( $X_{50} OY_{50}$ ) based on two backrests were established as Fig. 3. The X and Y coordinates of point  $P$  in  $C_{25}$  can be represented as  $[OB, PB]$ . Here the x-coordinate  $OB = PO \cos(\beta)$ , and the y-coordinate is computed as  $PB = PO \sin(\beta)$ , where  $PO = \sqrt{PA^2 + OA^2}$ ,  $\beta = 14 + \alpha$ , and  $\alpha = \tan^{-1} PA/OA$ . In  $C_{140}$ ,  $P$  is represented as  $[OC, PC]$ . Here  $OC = PO \cos(\gamma)$ , where  $\gamma = 39 + \alpha$ , and  $PC = PO \sin(\gamma)$ .

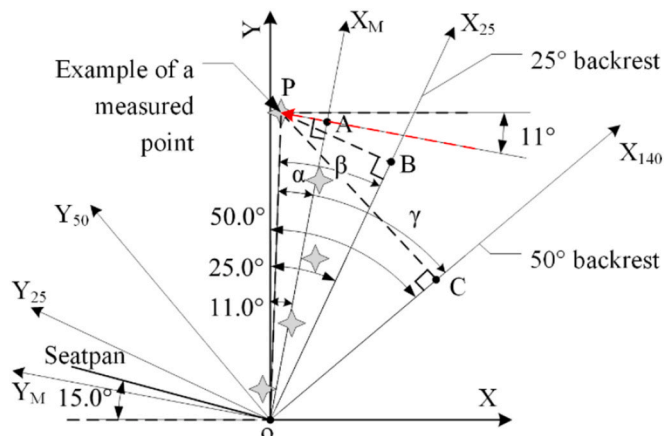


Fig. 3. Correction of measurement results- X – X-axis of World coordinate system;  $X_M$  - X-axis of  $CM$ ;  $X_{25}$  - X-axis of  $C_{25}$ ;  $X_{50}$  - X-axis of  $C_{50}$

For each subject in each setup ( $s = 0$  for  $25^\circ$  and  $s = 1$  for  $50^\circ$  setup),  $m = 3$  times the measurements were conducted, respectively. All measured points were translated to the corresponding coordinate system following the methods above. Then 3-degree splines were used to fit the results (Fig. 4), resulting in two sets of non-uniform rational b-spline (NURBS) curves  $SP^s = \{SP^{s,j}(u) | u \in (0, 1), s = [25, 50], j = 1.36\}$  for each participant in each setup, where  $u$  is the normalized parameter of the curve. Fig. 5(a) presents two sets of these curves. In Fig. 5(b), we aligned the Y-axis of  $C_{25}$  and  $C_{50}$  to Y-axis of the world coordinate (XOY) for a better comparison of two set of curves.

Given a set of 36 curves  $SP^{25} = \{SP^{25,j}(u) | u \in (0, 1), j = 1.36\}$  for the  $25^\circ$  setup, each can be discretized to a set of points as  $SP_D^{25} = [SP^{25,j}[i], i = [0, 1, 2 \dots n], j = 1.36]$ , where  $n$  is the number of points. A statistical shape model (SSM) of  $SP_D^{25}$  can be built based on principal component analysis (PCA) (Yang et al., 2021) as:

$$SP_{ssm}^{25} = SP_{D_{mean}}^{25} + \sum_{k=0}^{q^{25}} \gamma_k^{25} PC_k^{25}.$$

Here  $SP_{D_{mean}}^{25}$  denotes the mean model of  $SP_D^{25}$ .  $\gamma_k$  are the coefficients of  $PC_k$ , which are a number of uncorrelated principal components (PCs). Similarly,  $SP_{ssm}^{50}$ , which is the SSM of  $SP_D^{50}$ , and  $SP_{ssm}$ , which is the SSM of all curves in both  $25^\circ$  and  $50^\circ$  setups, can be denoted as:

$$SP_{ssm}^{50} = SP_{D_{mean}}^{50} + \sum_{k=0}^{q^{50}} \gamma_k^{50} PC_k^{50}$$

and

$$SP_{ssm} = SP_{D_{mean}} + \sum_{k=0}^q \gamma_k PC_k.$$

### 3. Results

Fig. 6 illustrates the mean models of the three SSMs for the  $25^\circ$  setup,  $50^\circ$  setup, and the combined setup. These mean models represent the average human back contours derived from the SSMs, highlighting

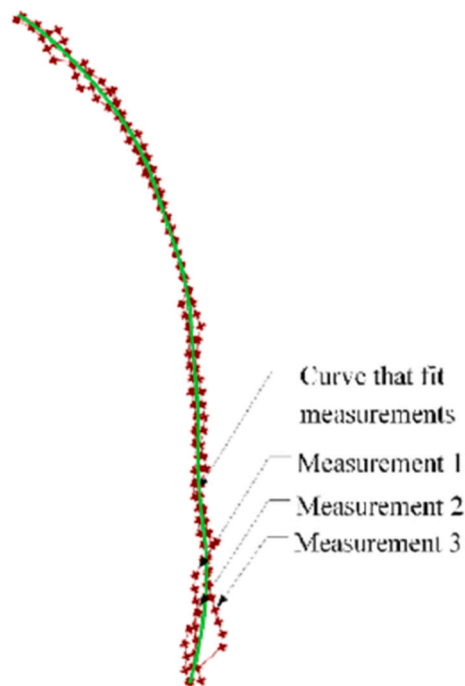


Fig. 4. Fitting 3 sets of measurement points with a 3-degree B-Spline curve for one participant.

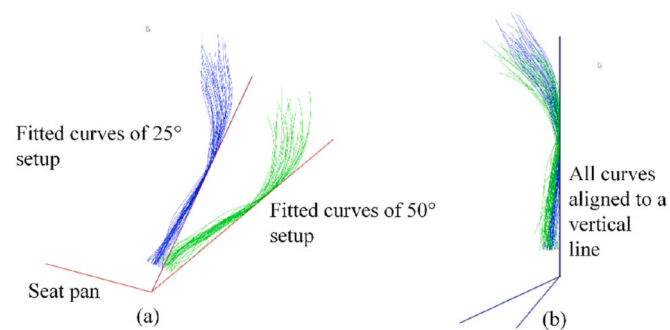


Fig. 5. (a) The interpolated curves in  $25^\circ$  (blue) and  $50^\circ$  (green) setups, (b) all curves aligned to a vertical line for analysis.

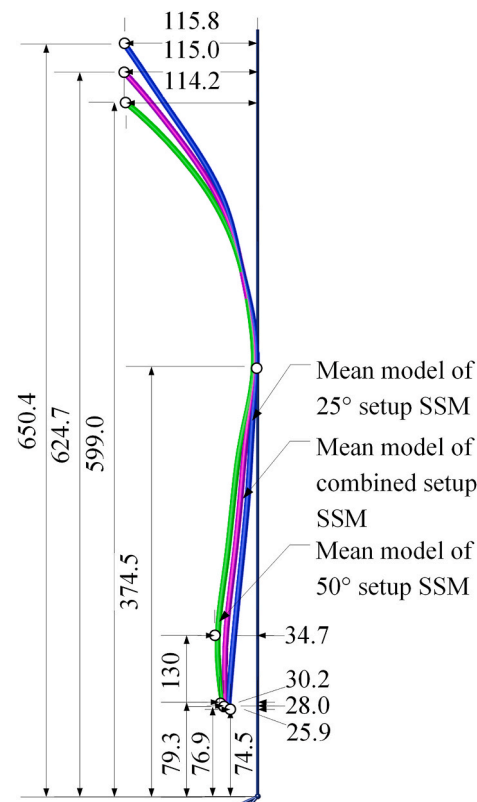


Fig. 6. Mean model of the  $25^\circ$ ,  $50^\circ$  and combined setups, distance unit in mm.

variations in back curvature across different backrest angles. In the mean model, the  $50^\circ$  setup demonstrates a more pronounced curvature, indicative of a relaxed and reclined posture, while the  $25^\circ$  setup shows a flatter curvature, consistent with an upright driving posture. The combined setup balances these two configurations, capturing the diversity in back shapes across both backrest angles.

For the top positions of the mean models, the  $25^\circ$  setup has a prominence of 115.8 mm from the backrest and 650.4 mm to the foam surface of the backrest. The  $50^\circ$  setup has a prominence of 114.2 mm from the backrest and 599.0 mm to the bottom of the backrest. The combined mean model lies in between, with a prominence of 115.0 mm from the backrest and 624.7 mm to the bottom of the backrest.

In the  $50^\circ$  setup, the prominence in the lumbar lordosis region reaches a maximum of 34.7 mm, positioned 130 mm above the seat pan level. At the same level above the seat pan, the prominence in the lumbar lordosis region of the combined setup and  $25^\circ$  setup are 28.0 mm and 21.3 mm, respectively. At 374.5 mm above the seat pan level, the prominence of the three curves regarding the backrest are the smallest.

Fig. 7 presents the compactness of the three SSMs, detailing the variance captured from PC1 to PC10 for each setup. The 25° setup consistently demonstrates the highest compactness across the components, capturing 79.7 % of the variance in PC1, 97.42 % by PC3, 99.06 % by PC5, and over 99.95 % by PC10, indicating that fewer components are required to represent the shape effectively. The 50° setup initially captures less variance, with 74.6 % in PC1, 96.02 % by PC3, 98.99 % by PC5, but converges to similar compactness levels (over 99.95 % by PC10). The combined setup balances the compactness of both individual setups, capturing 77.5 % in PC1, 96.61 % by PC3, 98.92 % by PC5, and over 99.95 % by PC10, suggesting that while it accommodates greater diversity, it retains reasonable compactness. These compactness trends highlight that the 25° setup yields the most compact representation of back shapes, likely due to the lower inter-subject variability typically observed in driving postures compared to the more relaxed and variable 50° setup, which will be further discussed in Section 4.2.

To further understand the pronounced curvature in the 50° setup compared to the 25° setup, we discretized the interpolated curves into 100 points to evaluate the accuracy of the mean models, as shown in Table 2. The mean direct Hausdorff distance, its standard deviation (std), and the Root Mean Square Error (RMSE) were calculated for each setup (Song et al., 2005). The 25° setup exhibited the lowest mean error ( $5.01 \pm 4.95$  mm) and RMSE (7.04 mm), reflecting a high degree of accuracy and consistency in representing the back shapes. In contrast, the 50° setup showed significantly higher errors, with a mean error of  $15.73 \pm 13.44$  mm and an RMSE of 20.70 mm, likely influenced by the variability in relaxed postures adopted by participants. The combined setup achieved a mean error of  $6.28 \pm 7.66$  mm and an RMSE of 9.91 mm, balancing the errors from both individual setups.

Fig. 8 presents the combined SSM along with the range of variability from PC1 to PC5, represented by  $\pm 3$  standard deviations (STD), covering 0.135 %–99.862 % of the total shape variation. In this model, PC1 primarily influences back height, PC2 captures variations in neck bending, and PC3 reflects differences in the lumbar lordosis region. For PC4 and PC5, the variations are smaller and less visually pronounced, indicating diminishing contributions to overall shape diversity.

In Fig. 9, the dimensions of the P5 to P95 back curves ( $\pm 1.645$  SD) based on PC1, PC2, and PC3 are presented. For the P5 to P95 range, the sitting height varies from 523.2 mm to approximately 726.1 mm, measured from the seat pan level. The maximum prominence difference in the lumbar lordosis region between P5 and P95 is 49.2 mm, located 134.1 mm above the seat pan. It is noteworthy that this prominence difference remains 36.9 mm even at a height of 250.4 mm above the seat pan, indicating consistent variability further up the back.

#### 4. Discussion

This study addressed two research questions: (1) What is the model of human back contour shapes in seated positions? (2) Can the model be

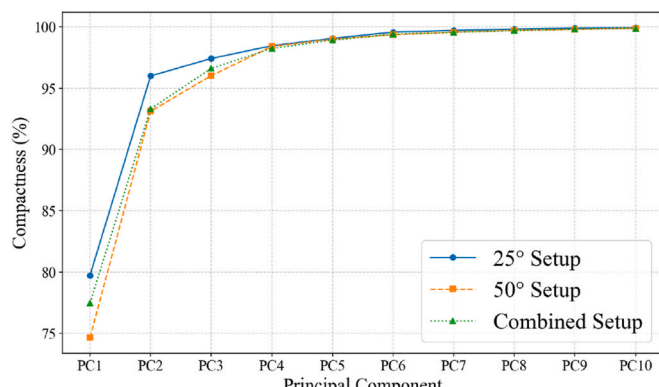


Fig. 7. Compactness of the model.

Table 2

Errors from the interpolated curves to the mean model.

	Mean error (mm)	RMSE (mm)
25° setup	$5.01 \pm 4.95$	7.04
50° setup	$15.73 \pm 13.44$	20.70
Combined setup	$6.28 \pm 7.66$	9.91

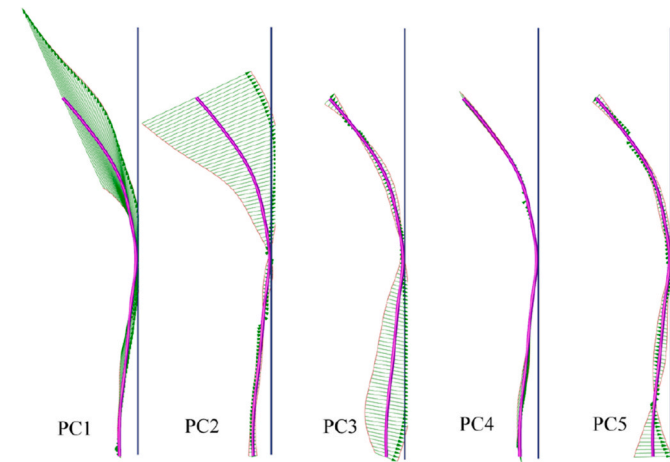


Fig. 8. The combined SSM illustrating the mean human back contour along with the range of variability represented by  $\pm 3$  STD.

extended to incorporate additional postures, such as sleeping, to better accommodate different NDRAs in automated vehicles? By developing SSMs and analyzing key shape parameters and their variations, this study presents new insights into human back contours in both seated and reclined postures.

#### 4.1. The SSM model

The SSMs generated in this study provide detailed geometric insights into back shapes across different postures. The principal components reveal how back-contour variability is distributed across the population. PC1 primarily reflects overall back height, representing the largest source of variation. PC2 captures cervical bending, highlighting differences in upper-spine alignment among participants. PC3 shows the greatest variation in the lumbar region, particularly in the area influenced by lumbar support. Together, these findings clarify how variations in back height, thoracic curvature, and lumbar prominence contribute to overall contour variability, providing critical input for specifying dimension zones in backrest design.

For the distance from C7 to the seat pan, the 25° setup measures 650.4 mm, the combined setup measures 624.7 mm, and the 50° setup measures 599.0 mm above the seat pan level in the mean models. The 50° setup is only slightly higher than the average sitting height (598 mm) in the Dutch population (Dined, 2011). However, C7 is generally positioned higher than the shoulder in the seated posture. This discrepancy might be due to: 1) In standard sitting height measurements, the seat pan angle is 0° and the backrest is vertical, with participants instructed to sit in an upright posture (Molenbroek et al., 2017). In contrast, in this study, the seat pan angle was 15°, and the backrest angle was either 25° (driving posture) or 50° (relaxed, reclined posture); 2) In this experiment, participants sat on a 6 cm thick foam cushion, and the resulting deformation was not accounted for. In contrast, anthropometric measurements are typically conducted with participants seated on a rigid wooden surface; and 3) The differences between the rotation centers of the participant's body and the seat backrest also contributed to discrepancies in the measured back contour.

Across all setups, the prominence of C7 regarding the backrest

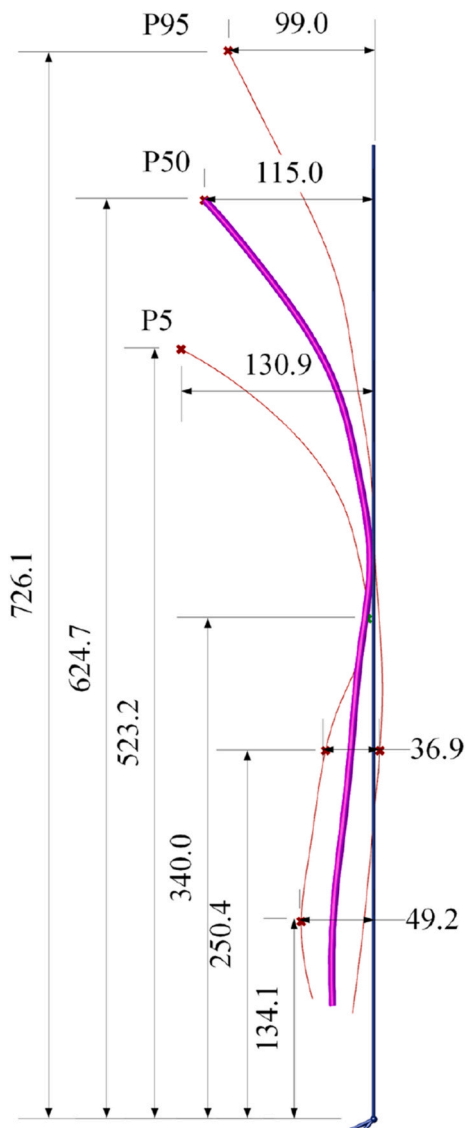


**Fig. 9.** Dimensions of the P5 to P95 human back contours generated by the model (in mm).

remains consistent at approximately 115 mm, aligning with values reported in existing literature. For instance, Kim et al. (2015) noted that the preferred pillow height for supporting the cervical region in reclining postures was approximately 10 cm, which closely corresponds to this measurement.

#### 4.2. Human back contours in seated postures

The results highlight the differences in human back contours between the 25° and 50° backrest setups. The mean models indicate that the 25° setup produces a flatter back contour, consistent with the upright posture typically associated with driving. In contrast, the 50° setup exhibits larger variations among all curves and generates a more pronounced back curvature, a finding that contrasts with previous literature (Andersson et al., 1979; Li et al., 2022). Specifically, the mean error of the SSM for the 50° setup is 15.73 mm, more than three times higher than the 5.01 mm observed in the 25° setup. The compactness analysis further supports these findings: the 25° setup demonstrates higher compactness, capturing 79.7 % of the variance in PC1, compared to 74.6 % in the 50° setup.

During the experiment, the absence of a fixed task in the 50°

(relaxed) condition allowed participants to adopt a wider range of natural postural behaviors, likely contributing to the greater variability observed. This reinforces the conclusion that human back contours in driving postures are relatively consistent, while those in relaxed positions are inherently more diverse. These insights underscore the importance of designing backrests that can adapt to a broader spectrum of user preferences and activities, particularly in automated vehicles, to ensure both stability and comfort across varied postures.

The differences between the 25° and 50° postures also have implications for human body dynamics. The more upright 25° posture, with its flatter and more compact back contour, supports a more stable pelvis-backrest interaction and results in more predictable load transfer through the spine during vehicle motions. In contrast, the greater curvature and variability observed in the 50° posture suggest reduced passive trunk stability and altered pelvis and torso kinematics, which may influence how occupants respond to braking or external disturbances. In current automotive practice, backrest recline is limited to approximately 40° because larger recline angles greatly increase the risk of submarining and loss of (3-point safety) belt-pelvis engagement (Boyle et al., 2019; Ressi et al., 2022). These dynamic and safety considerations further highlight the need for adaptable backrest designs and the exploration of alternative restraint concepts, e.g. five-point belt systems, that could safely support both upright and reclined postures in future vehicles.

#### 4.3. Design implications

##### 4.3.1. Backrest height

PC1 of the model indicates that the principal variation lies in the height of the back contours, making it a key consideration for backrest design. The dimensions of the P5 to P95 and P0.135 to P99.865 back curves provide actionable benchmarks, particularly regarding backrest height and adjustability. Fig. 9 suggests that the minimum height from C7 to the seat pan should be approximately 523.2 mm for the P5 population. Only for the P0.135 percentile, the back contour height reaches 439.7 mm. This supports findings from the literature (Nijholt et al., 2016), which emphasize that participant back shapes vary significantly from the commonly assumed 440 mm vertical distance from the seat pan.

Headrest adjustability becomes even more critical when accommodating a diverse population. To support users ranging from the P5 to P95 percentiles, the headrest must offer 202.9 mm of vertical adjustment to ensure proper head and neck support. This range enables optimal positioning for both shorter and taller individuals across different activities, such as relaxing or sleeping in automated vehicles.

##### 4.3.2. Possible hinge joint in the backrest

PC2 of the model reveals that the second-largest variation lies in the bending of the neck. Using the mean model for backrest design may result in a compromise in this area, as it does not fully accommodate the variability in neck curvature across individuals. An alternative approach could be to introduce a hinge joint at [0, 374.5] as shown in Fig. 6, allowing the backrest to adapt dynamically to these variations and better support different neck alignments. This adaptive feature could enhance user comfort, particularly for different NDRAs.

A three-vertex polyline, denoted as (PP1, PP2, PP3), was defined as illustrated in Fig. 9. This polyline was constructed within the bounding box of the target curves. One vertex (PP1) was placed on the top edge of the bounding box (as a parameter), another vertex (PP3) was located on the bottom edge (also as a parameter), and the third vertex (PP2, the hinge joint) was defined as [0, 374.5].

The best-fit polylines  $PP(PP1, PP2, PP3)$  were determined for the combined setup, where PP1 and PP3 were identified by minimizing the sum of squared distances between the polyline and each point in the relevant back curves  $P_{CM}^{s,i,m}$ . This optimization problem is represented

mathematically as:

$$PP(PP1, PP2, PP3) = \arg \min_{PP1, PP3} \sum_{j=0}^{72} \sum_{k=0}^n D(PP, P_{C_M}^{s.i.m})^2$$

where  $D$  is the Hausdorff distance calculated between  $PP$  and the  $n$  discretized back curves  $P_{C_M}^{s.i.m}$ . The results of this fitting are presented in Fig. 9 showing the dimensions of  $PP1$ ,  $PP2$ , and  $PP3$  with an RMSE of 17.73 mm. While an articulated region could theoretically allow the backrest to better follow these contour differences particularly during NDRAs such as reading or resting, this remains a geometric design implication rather than a validated comfort improvement. The actual comfort or usability benefits of such a hinge mechanism would need to be tested in future studies.

#### 4.3.3. Lumbar support

The third-largest variation in the model (PC3) occurs in the lumbar region. To accommodate the P5–P95 population, the model indicates that a lumbar support should provide approximately 49.2 mm of prominence when positioned around 134.1 mm above the seat pan level (Fig. 9). This required prominence exceeds the 30 mm recommendation by Carcone and Keir (2007), although their findings were based on upright office-chair postures rather than automotive seating.

In addition to prominence, the results show that lumbar support must span a broader vertical range. Specifically, the contour variation suggests that support may need to extend upward to roughly 250.4 mm above the seat pan, where a prominence of 36.9 mm is still needed (Fig. 9). These values are consistent with recommendations in earlier studies. For instance, Korte (2013) recommended a lumbar support height of  $192 \pm 31$  mm for office chairs, and Reed et al. (M. P. Reed et al., 1995) proposed a lumbar-support region covering approximately 120 mm in vertical extent. The extended vertical range observed in our model reinforces the need for adjustable or multi-segment lumbar

support in future automotive seating.

#### 4.4. Limitations and future directions

While this study advances our understanding of back shapes in seated positions, several limitations must be acknowledged. First, although the participant sample included a range of individuals, it was predominantly of young Western European origin. This may limit the generalizability of the findings to other populations with different anthropometric characteristics. For instance, the curvature of the cervicothoracic spine changes progressively with age (Boyle et al., 2002). Future studies should aim to include a more ethnically and geographically diverse sample to better capture the full spectrum of back contour variability. Furthermore, though we attempted to balance gender during recruitment, the limited number of participants prevents us from reporting reliable gender differences or conducting in-depth correlation analyses between anthropometric properties and back-contour features.

Additionally, this study focused solely on two static seated positions representing typical driving and relaxing/sleeping postures. While these postures provide valuable insights into back contours at specific backrest angles, there are further considerations: 1) The notion of an “ideal” sitting posture is still debated (Claus et al., 2009). The comfortable postures identified in the 50° setup were based on participants’ subjective preferences, which can vary significantly depending on the activity; 2) Dynamic measurements during transitions between postures could offer a more comprehensive understanding of how back contours evolve over time. Such transitions are important, as spinal curvature is known to adapt in response to changing postures.

The restricted range of backrest angles, limited to the 25° and 50° setups, also constrains the scope of the findings. Exploring a broader spectrum of angles could improve the adaptability of the SSM, enabling it to better accommodate a wider variety of postures and activities, particularly those encountered in automated vehicle scenarios. Furthermore, the absence of a headrest in the measurement setup represents another limitation. Headrests, as external interventions, can significantly influence back contours, especially in reclined postures. Their absence in this study, particularly in the 50° setup, may have contributed to participants’ difficulty in achieving a comfortable position. This, in turn, may have contributed to the greater variability observed in the back contours for the 50° setup. Meanwhile, a 7 cm offset from the seat pan meant the buttock region was not fully captured. Although the dataset includes the neck, shoulder, and lumbar areas, the role of buttock shape, potentially influencing PC3 and PC5, remains uncertain and warrants further study.

Additionally, while posture may influence static and dynamic comfort as well as motion sickness susceptibility, these effects were beyond the scope of the present geometric modelling study. Future research should investigate these comfort-related outcomes to provide a more complete understanding of the implications of reclined seating in future vehicles.

Lastly, the theoretical findings presented in this study should be evaluated in practical applications. Designing a backrest that follows the contour characteristics identified in this study is recommended, and future work should examine whether such designs improve perceived comfort or reduce discomfort compared to traditional seats.

#### 5. Conclusion

This study advances the understanding of human back contour shapes in seated and reclined positions through the development of SSMs. The findings reveal that the 25° backrest setup produces a flatter back contour, while the 50° setup shows greater variability and a more pronounced curvature. The combined setup balances these differences, offering a comprehensive model for diverse activities. Future research should include a more demographically diverse population and investigate the influence of headrests on back contour and perceived comfort,

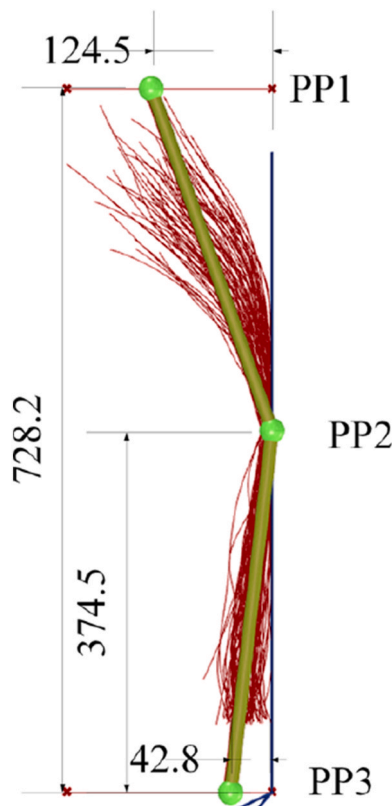


Fig. 9. The fitted polylines (units: mm).

especially in reclined postures relevant to automated vehicles.

## CRediT authorship contribution statement

**Anna Bokdam:** Writing – original draft, Visualization, Validation, Investigation, Formal analysis, Data curation, Conceptualization. **Gerbera Vledder:** Writing – review & editing, Methodology, Conceptualization. **Yu (Wolf) Song:** Writing – review & editing, Writing – original draft, Visualization, Validation, Supervision, Software, Resources, Project administration, Methodology, Investigation, Formal analysis, Data curation, Conceptualization. **Peter Vink:** Writing – review & editing, Validation, Supervision, Resources, Methodology.

## Ethical statement

The present research was approved by the Human Research Ethics Committee (HREC) of Delft University of Technology under file number 4717. Informed consent was obtained from all participants prior to their involvement in the study.

## Declaration of generative AI and AI-assisted technologies in the writing process

During the preparation of this work the author(s) used ChatGPT in order to review the English language usage. After using this tool/service, the author(s) reviewed and edited the content as needed and take(s) full responsibility for the content of the publication.

## Declaration of interest

The authors declare that they have no known competing financial interests or personal relationships that could have appeared to influence the work reported in this paper.

## References

Andersson, G.B., Murphy, R.W., Ortengren, R., Nachemson, A.L., 1979. The influence of backrest inclination and lumbar support on lumbar lordosis. *Spine* 4 (1), 52–58. <https://doi.org/10.1097/00007632-197901000-00009>.

Boyle, J.J.W., Milne, N., Singer, K.P., 2002. Influence of age on cervicothoracic spinal curvature: an ex vivo radiographic survey. *Clin. Biomed.* 17 (5), 361–367. [https://doi.org/10.1016/s0268-0033\(02\)00030-x](https://doi.org/10.1016/s0268-0033(02)00030-x).

Boyle, K.J., Reed, M.P., Zaseck, L.W., Hu, J., 2019. A human modelling study on occupant kinematics in highly reclined seats during frontal crashes. Proceedings of the International Research Conference on the Biomechanics of Impact, IRCOBI, Florence, Italy. 11th September–13th September. *IRC-19-43*. <https://www.scopus.com/inward/record.uri?eid=2-s2.0-8506605389&partnerID=40&md5=7558e1baac1397fe3b582c004d5dde1a>.

Cai, Y., Anjani, S., Withey, D., Vledder, G., Song, Y., Vink, P., 2024. Changes in non-driving-related activities from conditional to full automation and their implications for interior design: a systematic review and meta-analysis. *Applied Sciences* (Basel, Switzerland) 14 (20), 9442. <https://doi.org/10.3390/app14209442>.

Carcone, S.M., Keir, P.J., 2007. Effects of backrest design on biomechanics and comfort during seated work. *Appl. Ergon.* 38 (6), 755–764. <https://doi.org/10.1016/j.apergo.2006.11.001>.

Claus, A.P., Hides, J.A., Moseley, G.L., Hodges, P.W., 2009. Is “ideal” sitting posture real? Measurement of spinal curves in four sitting postures. *Man. Ther.* 14 (4), 404–408. <https://doi.org/10.1016/j.math.2008.06.001>.

Claus, A.P., Hides, J.A., Moseley, G.L., Hodges, P.W., 2016. Thoracic and lumbar posture behaviour in sitting tasks and standing: progressing the biomechanics from observations to measurements. *Appl. Ergon.* 53 (Pt A), 161–168. <https://doi.org/10.1016/j.apergo.2015.09.006>.

de Oliveira, T.S., Candotti, C.T., La Torre, M., Pelinson, P.P.T., Furlanetto, T.S., Kutchak, F.M., Loss, J.F., 2012. Validity and reproducibility of the measurements obtained using the flexicurve instrument to evaluate the angles of thoracic and lumbar curvatures of the spine in the sagittal plane. In: *Rehabilitation Research and Practice*, 2012, 186156. <https://doi.org/10.1155/2012/186156>.

Dined, 2011. DINED anthropometric database. Dined.NL. <http://dined.io.tudelft.nl/ergonomics/>.

Franz, M., Kamp, I., Durt, A., Kilincsay, U., Bubb, H., Vink, P., 2011. A light weight car seat shaped by human body contour. *Int. J. Hum. Factors Model Simulat.* 2 (4), 314–326. <https://doi.org/10.1504/IJHFMS.2011.045002>.

Hiemstra-van Mastrigt, S., Smulders, M., Bouwens, J.M.A., Vink, P., 2019. Chapter 61 – designing aircraft seats to fit the human body contour. In: Scataglini, S., Paul, G. (Eds.), *DHM and Posturography*. Academic Press, pp. 781–789. <https://doi.org/10.1016/B978-0-12-816713-7.00061-1>.

Kaiser, J.T., Reddy, V., Launico, M.V., Lugo-Pico, J.G., 2024. Anatomy, head and neck: cervical vertebrae. In: *Statpearls*. StatPearls Publishing. <https://www.ncbi.nlm.nih.gov/books/NBK539734/>.

Kandasamy, G., Bettany-Saltikov, J., van Schaik, P., 2021. Posture and back shape measurement tools: a narrative literature review. In: *Spinal Deformities in Adolescents, Adults and Older Adults*. IntechOpen. <https://doi.org/10.5772/intechopen.91803>.

Kim, H.C., Jun, H.S., Kim, J.H., Ahn, J.H., Chang, I.B., Song, J.H., Oh, J.K., 2015. The effect of different pillow heights on the parameters of cervicothoracic spine segments. *Korean Journal of Spine* 12 (3), 135–138. <https://doi.org/10.14245/kjs.2015.12.3.135>.

Korte, J., 2013. *South African Anthropometric Dimensions for the Design of an Ergonomic Office Chair*. Rhodes University [Master's thesis].

Li, C., Zhao, Y., Yu, Z., Han, X., Lin, X., Wen, L., 2022. Sagittal imbalance of the spine is associated with poor sitting posture among primary and secondary school students in China: a cross-sectional study. *BMC Musculoskelet. Disord.* 23 (1), 98. <https://doi.org/10.1186/s12891-022-05021-5>.

Meakin, J.R., Gregory, J.S., Aspden, R.M., Smith, F.W., Gilbert, F.J., 2009. The intrinsic shape of the human lumbar spine in the supine, standing and sitting postures: characterization using an active shape model. *J. Anat.* 215 (2), 206–211. <https://doi.org/10.1111/j.1469-7580.2009.01102.x>.

Molenbroek, J.F.M., Albin, T.J., Vink, P., 2017. Thirty years of anthropometric changes relevant to the width and depth of transportation seating spaces, present and future. *Appl. Ergon.* 65 (Suppl. C), 130–138. <https://doi.org/10.1016/j.apergo.2017.06.003>.

Naddeo, A., Morra, A., Califano, R., 2024. Human-centered design and manufacturing of a pressure-profile-based pad for better car seat comfort. *Machines* 12 (6), 374. <https://doi.org/10.3390/machines12060374>.

Nijholt, N., Tuinhof, T., Bouwens, J.M.A., Schultheis, U., Vink, P., 2016. An estimation of the human head, neck and back contour in an aircraft seat. *Work* 54 (4), 913–923. <https://doi.org/10.3233/WOR-162355>.

Reed, M.P., Ebert, S.M., Jones, M.L.H., Hallman, J.J., 2020. Prevalence of non-nominal seat positions and postures among front-seat passengers. *Traffic Inj. Prev.* 21 (Suppl. 1), S7–S12. <https://doi.org/10.1080/15389588.2020.1793971>.

Reed, M.P., Schneider, L.W., 1996. Lumbar support in auto seats: conclusions from a study of preferred driving posture. *SAE Technical Paper Series*, Article 960478. International Congress & Exposition. <https://doi.org/10.4271/960478>.

Reed, M.P., Schneider, L.W., Eby, B.H., 1995. The Effects of Lumbar Support Prominence and Vertical Adjustability on Driver Postures. University of Michigan. <https://deepblue.lib.umich.edu/handle/2027.42/1113?show=full>.

Ressi, F., Leo, C., Klug, C., Sinz, W., 2022. Protection challenges in seat positions with large rearward adjustment in frontal collisions: an approach using stochastic human body model simulations. *Frontiers in Future Transportation* 3, 914481. <https://doi.org/10.3389/futtr.2022.914481>.

Song, R., Vergeest, J.S.M., Bronsvort, W.F., 2005. Fitting and manipulating freeform shapes using templates. *J. Comput. Inf. Sci. Eng.* 5 (2). <https://doi.org/10.1115/1.1875592>.

Tsagkaris, C., Widmer, J., Wanivenhaus, F., Redaelli, A., Lamartina, C., Farshad, M., 2022. The sitting vs standing spine. *N. Am. Spine Soc. J.* 9 (100108), 100108. <https://doi.org/10.1016/j.xnsj.2022.100108>.

Varela, M., Gyi, D., Mansfield, N., Picton, R., Hirao, A., Furuya, T., 2019. Engineering movement into automotive seating: does the driver feel more comfortable and refreshed? *Appl. Ergon.* 74, 214–220. <https://doi.org/10.1016/j.apergo.2018.08.024>.

Vink, P., Vledder, G., Smulders, M., Song, Y., 2025. How do we sleep? Towards physical requirements for space and environment while travelling. *Appl. Ergon.* 122 (104386), 104386. <https://doi.org/10.1016/j.apergo.2024.104386>.

Vledder, G., Sabater Compomanes, R., Singh, U., Kılıç, H., Smulders, M., Song, Y., Vink, P., 2024. Experiences of upright sleeping in a vehicle: the preferred back rest angle. *Advances in Human Factors of Transportation* 148. <https://doi.org/10.54941/ahfe1005258>.

Voinea, G.-D., Butnariu, S., Mogan, G., 2016. Measurement and geometric modelling of human spine posture for medical rehabilitation purposes using a wearable monitoring System based on inertial sensors. *Sensors* 17 (1). <https://doi.org/10.3390/s17010003>.

Wiyanad, A., Amatachaya, S., Suwannarat, P., Chokphukiao, P., Sooknuan, T., Gaogasigam, C., 2023. The seventh cervical vertebra is an appropriate landmark for thoracic kyphosis measures using distance from the wall. *Wu Li Chih Liao [Hong Kong Physiotherapy Journal]* 43 (1), 43–51. <https://doi.org/10.1142/S1013702523500038>.

Yang, Y., Yuan, T., Huysmans, T., Elkhuizen, W., Tajdari, F., Song, Y., 2021. Posture-invariant 3D human hand statistical shape model. *J. Comput. Inf. Sci. Eng.* 21. <https://doi.org/10.1115/1.4049445>.

Zemp, R., Taylor, W.R., Lorenzetti, S., 2013. In vivo spinal posture during upright and reclined sitting in an office chair. *BioMed Res. Int.* 2013 (1), 916045. <https://doi.org/10.1155/2013/916045>.